Available online at www.asric.org

ASRIC Journal on Natural Sciences 1 (2022) 14-35

# Spacecraft Attitude and Orbit Determination from the Cost and Reliability Viewpoint: A Review

Tamer Mekky[1], Ahmed Habib

[1]National Authority for Remote Sensing and Space Science, Cairo, Egypt

Corresponding Authors Email: tamermekky@hotmail.com

Received 28 May 2021; revised 31 June 2021; accepted 20 August 2022

***Abstract* – Spacecraft attitude and orbit control subsystem (AOCS) is responsible for about 30% of the failures of spacecraft. Spacecraft Attitude and orbit determination (SAOD) are two main tasks which are executed by an AOCS. For some spacecraft missions, mission success criterion is related directly to the performance of AOCS. A typical SAOD process is composed from software and hardware. SAOD software has many functions such as management of normal and abnormal operation, in addition to state estimation. SAOD hardware is composed from various sensors, processors, and peripherals. Thus, calculating and increasing the reliability of these interconnected components is a real challenge taking into account the constraints associated with AOCS design. These constraints contain and not limited to high reliability, limited processing power, overall subsystem mass, overall subsystem cost, and limited electric power capabilities. Thus, to increase system reliability against failures, subsystem cost should be carefully considered and minimized. The current article reviews the methods of SAOD in addition to reliability and cost associated with it.**

***Keywords* – Spacecraft, Attitude, Orbit, Cost, reliability.**

## I. INTRODUCTION

The spacecraft attitude and orbit control subsystem (AOCS) is considered to be one of the critical subsystems those directly affecting the spacecraft mission performance. Formally, this subsystem is responsible for providing four tasks. They are namely: Spacecraft attitude monitoring, Spacecraft orbit monitoring, Spacecraft attitude control, and finally Spacecraft orbit control. The first three tasks are usually done over all of the spacecraft flown till today, while as the fourth task may or may not exist onboard a spacecraft. This is because of the reason that many spacecraft are designed without the ability of orbit control. The tasks of spacecraft attitude and orbit monitoring are considered to be the main subjects of the current review article. The task of spacecraft attitude and orbit control is not considered herein. The task of spacecraft attitude and orbit monitoring requires some form of integration among hardware and software components. A block diagram of such components is shown in Fig. 1.

Reliability is defined as “The probability that a device will function without failure over a specific time period or amount of usage.” [1], [2]. The basic reliability is defined as “The probability that a device will function without failure of any kind over a specific time period or amount of usage”. Another definition of reliability is that “The probability that the system will function as expected” [3].

Spacecraft subsystems such as AOCS tend to be relatively expensive or extremely complex, or both. In addition, in most cases, they are not repairable. This is because of the reason that, once the spacecraft goes into space, it never comes back again for repair. Hence, the AOCS onboard a 3-axis stabilized spacecraft is required to be reliable. Usually, the AOCS is considered to be of crucial importance for on-orbit operation [4]. Its degradation can greatly affect the whole spacecraft operation, and may lead to mission failure. The tasks of attitude and orbit monitoring are usually two main tasks implemented by the AOCS.

Cost effectiveness of a reliable AOCS is thought to be a challenge. There are several methods of cost estimation and cost reduction. These methods are discussed in a subsequent section. These methods are discussed within the framework of faster, cheaper, and better paradigm.

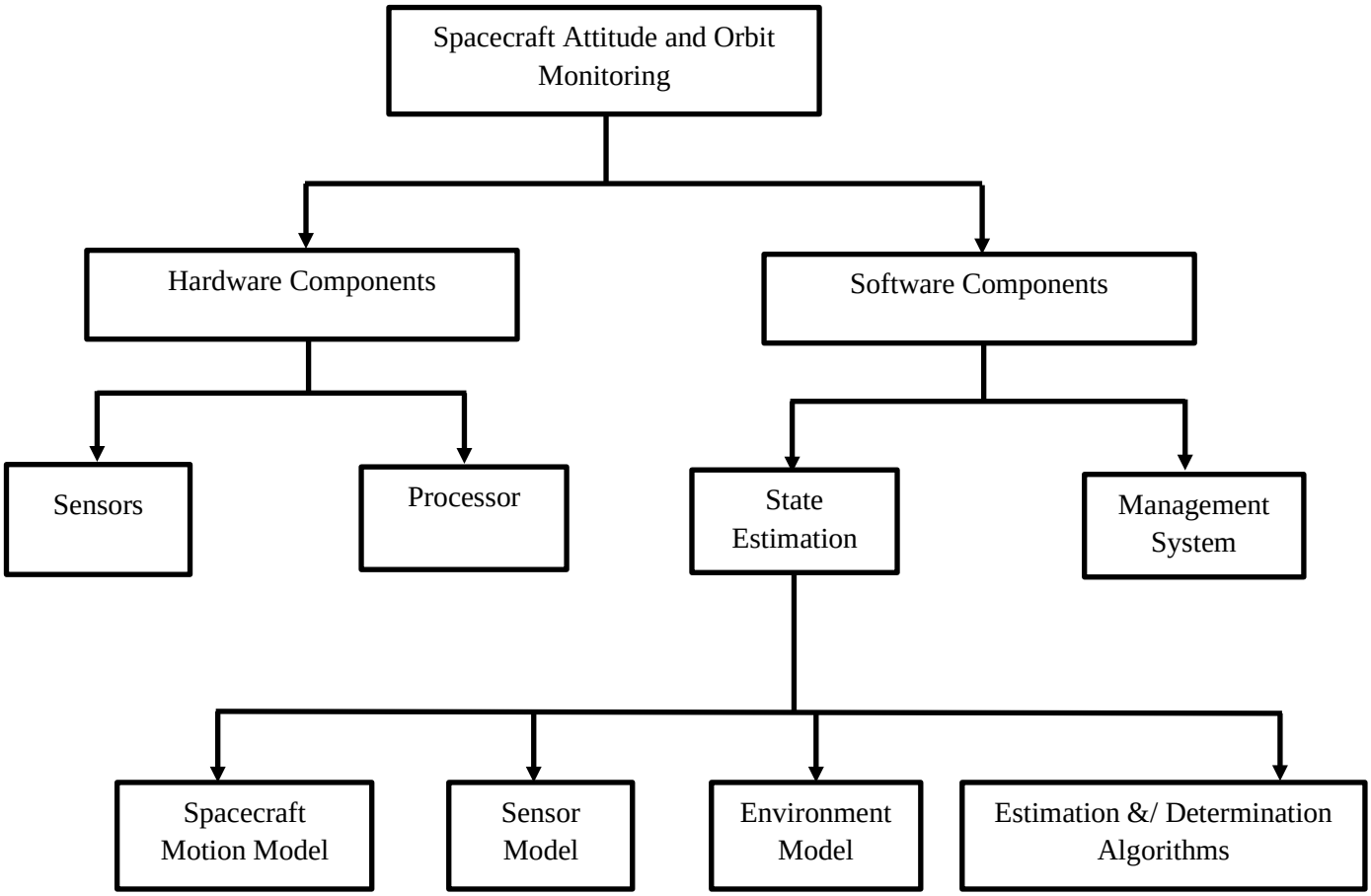


Fig. 1. Components of a typical attitude and orbit monitoring system.

The structure of this review paper is organized as follows: First a description of AOCS, and its components is reviewed. Second, a review over reliability concepts and mathematics is presented. Since the definition of reliability is related to the probability, some knowledge of probability theory is essential [3]. Third, Methodologies of spacecraft attitude and orbit monitoring cost effectiveness are presented. In addition, case studies are given according to the flow of information.

## II. ATTITUDE AND ORBIT MONITORING HARDWARE COMPONENTS

Any spacecraft flying in orbit exhibits three kinds of motions. The first kind of motions is the translational motion. In this kind of motion, the spacecraft is translated without any rotation from one place to another. This motion is commonly known as orbital motion. The second kind of motions is the rotation of the spacecraft around one or more of its body axes. This motion is commonly known as the attitude motion. These rotations could be expressed in different forms such as, Euler angles, Euler-axis angle, quaternion vector, and Rodriguez parameters. In the current review article we will select the Euler angles and the quaternion vector representations of spacecraft attitude. Euler angles are three independent rotations about the three spacecraft body axes which are shown in Fig. 2.

The rotation about the spacecraft x-axis is commonly known as the roll angle, about the y-axis is commonly known as the pitch angle, and about the yaw angle is commonly known as the yaw angle. Expression of spacecraft rotational motion in terms of Euler angles usually suffers from singularities at specific angles according to the rotation sequence assumed. Because of this mathematical problem, the quaternion vector is used instead. The third kind of motions is a mix of the former two kinds. Usually, the study of spacecraft orbital motion is separated from the study of spacecraft attitude motion. [5], [6], and [7] are standard text books those completely cover the orbital motion. Ref. [8] is also a standard text book that covers completely the attitude motion of the spacecraft. [9], [10], [11], [12], [13], [14], [15], [16], and [17] deal with the combined orbital and attitude motion of the spacecraft. The task of the AOCS is to monitor and control both motions based on different types of measurements and actuators.

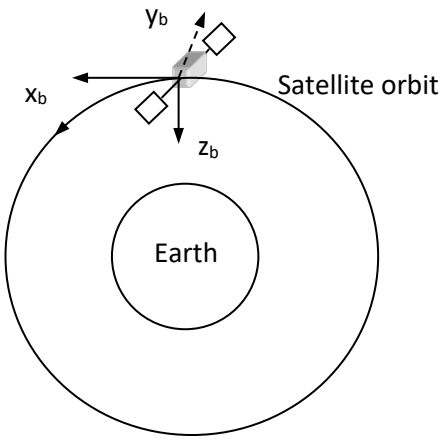


Fig. 2. Spacecraft body axes.

The current review paper considers only the monitoring job of the spacecraft attitude and orbital motion. There are several kinds of sensors. Some of these sensors measure directly the desired quantities and others do not do so. Spacecraft sensor are divided into spacecraft attitude motion sensors, spacecraft orbital motion sensors, and dual usage sensors which could be used as attitude and orbital motion sensors. Each type of sensors is discussed below

**2.1 Sensors**

**2.1.1 Spacecraft attitude motion sensors**

I- Magnetometers: Magnetometers are devices those measure the earth's magnetic field vector direction and magnitude. Magnetometers are widely used sensors nearly onboard every spacecraft. They are characterized by the absence of any moving parts. This in turn increases their reliability. The reliability of the magnetometer used onboard the former egyptian satellite EGYPTSAT-1 is 0.9978 for 3 years and 0.9939 for 5 years [18]. In addition, magnetometers are also characterized by low power consumption, light weight, and operability over a wide range of temperatures. One of the main disadvantages of the magnetometer is that it is not accurate due to several reasons. Magnetometers have wide range of applications nowadays, you may be having one of them inside your cellular phone. It could be in the form of a very small Integrated Circuit (IC) board as shown in Fig. 3 [19]. Magnetometers have various types such as: search-coil magnetometer (passive and active), flux-gate magnetometer, optically-pumped magnetometer, nuclear (proton)-precession magnetometer, superconducting quantum interference device, Hall-effect magnetometer, Magnetoresistive magnetometer, Magnetodiode magnetometer, Magnetotransistor magnetometer, Fiberoptic magnetometer, and Magnetoptical magnetometer [20].


Fig. 3. 3-Axis Digital Compass Magnetometer Module.


Fig.4. Sun Sensor.

II- Sun sensors: This sensor senses the direction of the sun in the spacecraft body axes. There are several kinds of sun sensors such as analog sun sensors, sun presence sensors and digital sun sensors. A major drawback of this sensor is its intermittent operation due to the absence of the sun or shadowing caused by other spacecraft components. A sample model of a sun sensor is given in Fig. 4 [21].

III- Horizon sensors: Horizon sensors are devices which could be used to determine the orientation (attitude) of the spacecraft relative to the earth. This type of sensors has an optical system. Horizon sensors also could be used to determine only two attitude angles out of three. Sometimes, horizon sensors are named as earth horizon sensor, or even earth sensor. Fig.5 [3] shows a picture for an earth horizon sensor [22].

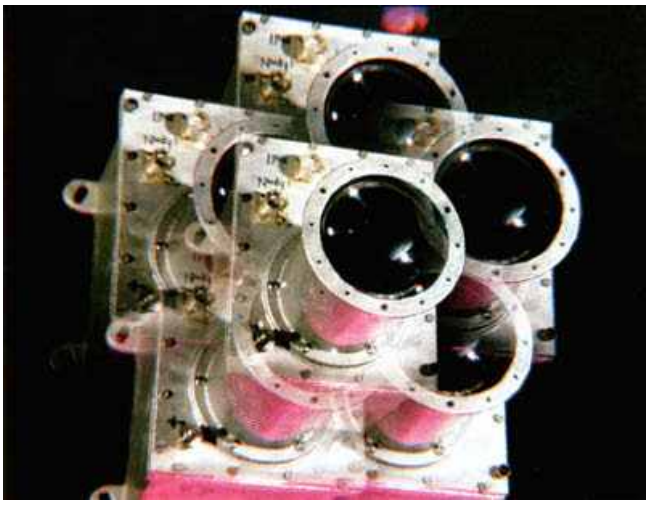

Fig. 5. Earth horizon sensor.

IV- Moon sensor: This sensor is developed by Mortari, D. This sensor is based on the idea of capturing an image of the moon, and by means of image processing spacecraft orientation could be inferred [23]. It is not a common sensor. The image of the moon is captured by a low-cost charge-coupled device camera.

V- Gyroscopes: Gyros are instruments those could provide angular measurements. These angular measurements could be either the angular velocities or the angular displacements according to gyro type. If the instrument provide only angular velocity it is called rate gyro. If it could provide angular displacement it is called rate integrating gyro. Traditionally, when the word “gyro” is used it is meant that it is a rate gyro. There is a third type of gyros called control moment gyros which generate torque to control the spacecraft attitude. But this type of gyros is out of scope for the current review article. A traditional mechanical gyros consists of a spinning mass mounted to a base. The spinning axis tends to be inertially fixed and any rotational movement of the base at which the spinning mas is attached could be measured with respect to the fixed inertial axis. Technology advancement enabled the existence of other kinds of gyroscopes such as Fiber Optic Gyros (FOG), and microelectromechanical systems (MEMS) gyros. All of the Fiber optic gyros are based on Sagnac effect. When two identical light waves travel along a fiber optic circular path which is slowly rotating arrive at the end of the path with phase difference between each other. This phase difference could be measured with an interferometer. The measured phase shift is directly proportional to the angular velocity to be measured. Fig. 6. Shows a sample Fiber Optic Gyro. This FOG has a mass of 10 kg and a reliability greater than 0.995 over 5

years of continuous operation. A MEMS gyro is a vibratory gyroscope which detects coriolis acceleration of a proof mass due to the induced rotation [24]. The accuracy of MEMS gyroscope is not so good compared to inertial grade sensors.

Fig. 6. A sample FOG.

VI- Star sensor: star sensor is the most accurate and expensive attitude sensor onboard a spacecraft. In addition, star sensors are characterized by heavy weight and high power compared to other spacecraft attitude sensors. Moreover, star sensors could not work at all when the sun falls inside or nearby its field of view due to the high illumination of the sun, typically within 30 to 60 deg of the sun direction. Additionally, star sensors could only be used when the spacecraft angular velocities are very low because high angular velocities causes the star images to be smear [25]. The last thing to point out is that star sensors are very complex devices. This complexity reduces their reliability considerably. Typical reliability values of such sensors are 0.95 over 15000 hour. A star sensor measures the star coordinates in the spacecraft body frame. Then it compares these coordinates with reference star directions acquired from a catalog of stars. The optical part of the sensor is used to capture an image of a set of stars. Then, this image is processed by the onboard star sensor to determine the position of stars, the brightness of the star, and other relevant information. The resulting processed information is then compared to a built-in catalog of stars to identify certain star pattern, or patterns. There are so many star identification techniques such as discrete attitude variation (lost-in-space), direct matching, phase matching, angular separation matching, and k- vector. The lost-in-space algorithm is a search algorithm that uses extensive processing because it does not need knowledge of the initial attitude. So, this algorithm is used only as a last resort. The process of star identification consumes a lot of time and computational resources. Star sensor classes are divided into three main classes: fixed head star tracker, gimbaled star tracker, and star scanners. Fixed head star trackers have electronic tracking and searching capabilities for a limited field of view. Gimbaled star trackers search and acquire stars based on their gimbaled mounts. Star scanners utilize the rotation of the spacecraft to provide star scanning process [8]. Fig. 7 shows an image of the engineers working on a star tracker [26].

Fig. 7. Star tracker.

**2.1.2 Orbital motion sensors**:

A well known sensor that is commonly used nowadays is Global Positioning System (GPS) receiver. The global positioning system is an integrated system that was originally developed to provide time information and location for earth, and near earth based users. The system was originally provided by the United States Department of Defense (DoD) for civilian and military applications. This system is operated and maintained by the USA and it is freely available for anyone equipped with a GPS receiver [27]. The system consists of three

segments [9]: The space segment, the control segment, and the user segment. The space segment consists of all the satellites constituting the GPS. The number of satellites revolving around the earth was originally 24 satellites distributed over six orbital planes in a sun-synchronous orbit of 20000 km altitude approximately. Each orbital plane is inclined 55$^{o}$ to the equatorial plane. The number of operational satellites nowadays is 32 satellites. A schematic diagram of the GPS constellation satellites is shown in Fig. 8 [28]. This constellation provides positioning and timing services. Each satellite has a very accurate atomic cesium clock with predictable or a known offset. Each satellite transmits its information over two L-band frequencies. The control segment consists of a number of ground control stations distributed around the globe. The master ground control station is located near Clorado Springs. These ground control stations provide continuous tracking for the entire constellation, maintain them in orbit, and upload necessary information. The master control station figures out the corrections those are uploaded to the constellation. The user segment consists of a GPS receiver that receives constellation information and performs some calculations to compute the user position. To be able completely to provide user position, at least four GPS satellites must be viewed simultaneously. There are also some navigation systems provided by Russia, China, and European Union countries. The Global Navigation Satellite Systems (GNSS) consists of integration between more than one of the navigation systems.

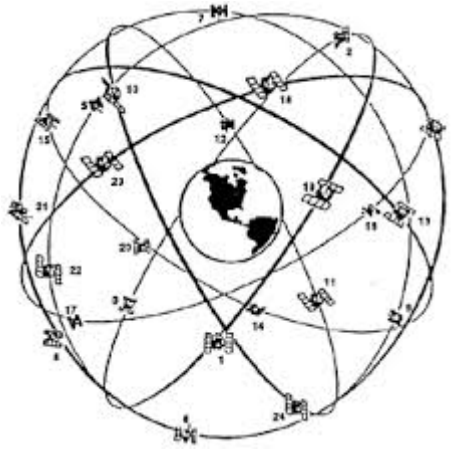

Fig. 8. GPS constellation.

GPS receiver can determine its position by measuring the range between it antenna and at least four GPS satellites. The signal broadcasted by each satellite contains the start time of broadcasting and travels from the GPS satellite to the receiver with the speed of light which could be approximated as a constant value. The distance travelled by the signal could be computed if its arrival time is recorded. At least four satellites (i.e., four distance measurements) are needed to determine the user 3-D position and time offset. Ref. [29] contains survey over some of the algorithms which are utilized to solve mathematically the positioning problem. These algorithms were the direct solution, improved direct solution, and improved direct solution based iterative solution.

Ground based orbital motion sensors: These sensors are normally mounted on the ground stations. These sensors include Laser retro-reflectors, dual doppler receivers, and optical observations [6]. The sensor operation periods last only for few minutes during which the spacecraft falls into the ground station field of view. Thus, these sensors are considered to be intermittent.

**2.1.3 Dual usage sensors**:

These sensors have the ability to be used as an orbital motion sensor or attitude motion sensor or both. These sensors are basically the magnetometer and GPS receivers.

*2.3.1 Magnetometer*: A magnetometer measures the earth's magnetic field vector. This measurement is a function of spacecraft orbital and attitude states. Thus, attitude and orbit information could be inferred. The inference process is very complex and suffers from several drawbacks. One of the drawbacks that ref. [30] suffered from is that there exist multiple solutions for the mathematical problem, because the problem is purely formulated. The earth's magnetic field vector magnitude draws contour lines over the earth. This means that several positions could have the same magnitude of the earth's magnetic field. This is the true reason of algorithm divergence. If the problem is formulated in a good way, you could converge to a solution within one or more orbital period after using a proper estimation algorithm. You could not get an instantaneous solution. This is because of that the number of states to be estimated are 12 or even more while as you have only 3 measurements corresponding to the three components of the earth's magnetic field. Of course, the observability

is enhanced if the sensor is aided with other attitude sensors. But still, the computational effort to deduce position information from magnetometer measurements is huge. This difficulty could be alleviated by current development of processing power.

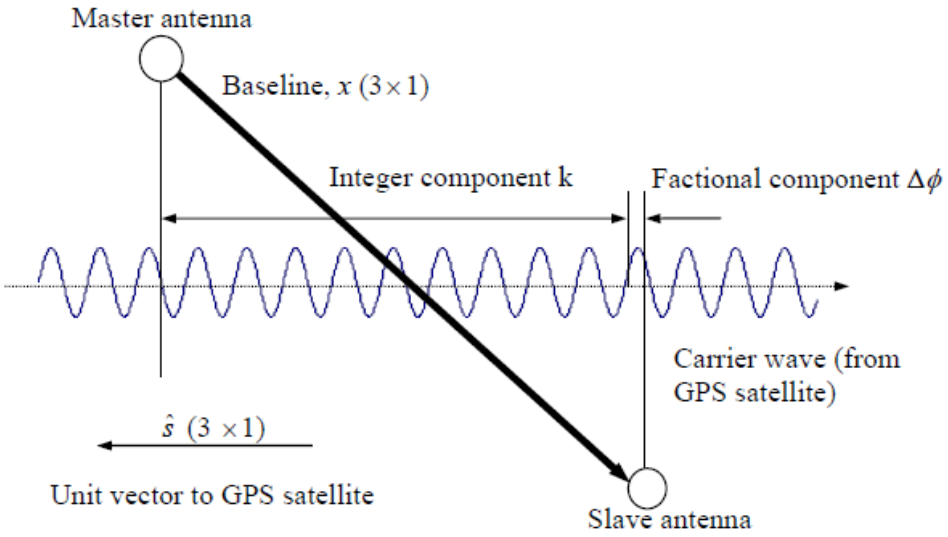


Fig. 9. Attitude motion observation geometry.

*2.3.2. GPS*: The second sensor that could be used for attitude and orbit monitoring is the GPS receiver [9], [30]. The idea of using the GPS signal to determine the attitude motion is shown in Fig. 9. The signal from GPS satellite arrives at two antennas, a master antenna and its accompanying slave. The receiver could measure the phase difference between the two antennas and this difference is a function of spacecraft attitude. To be able to completely solve the ambiguity, four antennas are required. Two major drawbacks arise fro using GPS receiver as an attitude sensor. The first drawback is that the cost of the receiver which is able to provide phase difference data is very high (typically exceeds 300 K $). The second drawback is that this method could be used only for long baselines (over 1 or two meters). Thus, it is very difficult to use such receiver onboard the class of Micro and Nano-satellites.

There are also some other sensors those could be used such as accelerometers, and Inertial Measurement Units (IMU), but these sensors don't have proven flight record.

**Case study**

The case study spacecraft is assumed to have many of the aforementioned sensors. The magnetometer is utilized as a dual usage sensor for both orbit and attitude monitoring. The gyro and the star sensor are used for attitude monitoring. A GPS receiver is utilized to provide position measurements. The initial parameters of the case study spacecraft are $a$ (semi major axis) = 7257200 m, $e$ (orbit eccentricity) = 0, $i$ (orbit inclination) = 98.085°, $\Omega$ (right ascension of ascending node) = 337°, $\omega$ (argument of perigee)= 60° °, $\upsilon$ (true anomaly)=3°, $\phi$ (roll angle)= □160°, $\psi$ (yaw angle)= 150° , and $\theta$ (pitch angle)= □□° .The estimated satellite parameters are initialized with $a$ (semi major axis) = 7057200 m, $e$ (orbit eccentricity) = 0, $i$ (orbit inclination) = 88.28°, $\Omega$ (right ascension of ascending node) = 339°, $\omega = 70$ °, and $\upsilon = 0$ °, $\phi$ (roll angle)= □°, $\psi$ (yaw angle)= 0° , and $\theta$ (pitch angle)= □°. Epoch time (1/4/2013 0h:0m:0s). Time step ( $\Delta T$ ) = 4 seconds. The continuous measurement noise covariance matrix is given by

$$R = \begin{bmatrix} R_{11} & 0_{3*3} & 0_{3*4} & 0_{3*3} \\ 0_{3*3} & R_{22} & 0_{3*4} & 0_{3*3} \\ 0_{4*3} & 0_{4*3} & R_{33} & 0_{4*3} \\ 0_{3*3} & 0_{3*3} & 0_{3*4} & R_{44} \end{bmatrix}$$

With

$$R_{11}=\left(\frac{50}{3}\times 10^{-9}\right)^2 I_{3\times 3},\quad R_{22}=\left(\frac{0.02}{3}\times\frac{\pi}{180\times 60\times 60}\right)^2 I_{3\times 3},\quad R_{33}=\left(\frac{0.000484814}{3}\right)^2 I_{4\times 4},\quad \text{and}$$

$$R_{44}=\left(\frac{50}{3}\right)^2\times I_{3\times 3}$$

The continuous process noise covariance matrix is given by

$$Q=\begin{bmatrix} Q_{11} & 0_{6\times 7} \\ 0_{7\times 6} & Q_{22}\end{bmatrix}$$

Where

$$Q_{11}=\begin{bmatrix} Q_{33} & 0_{3\times 3} \\ 0_{3\times 3} & Q_{44}\end{bmatrix},\qquad Q_{33}=\left(30\times 10^3\right)^2\times I_{3\times 3},\qquad \text{and}\qquad Q_{44}=26^2 I_{3\times 3},\qquad Q_{22}=\begin{bmatrix} Q_{55} & 0_{4\times 3} \\ 0_{3\times 4} & Q_{66}\end{bmatrix},$$

$$Q_{55}=\left(0.001\times\frac{\pi}{180}\right)^2\times I_{4\times 4},\ Q_{66}=\left(5\times 10^{-5}\right)^2\times I_{4\times 4},$$

The initial estimation error covariance matrix is given by

$$P_0=\begin{bmatrix} P_{11} & 0_{6\times 7} \\ 0_{7\times 6} & P_{22}\end{bmatrix}$$

Where

$$P_{11}=\begin{bmatrix} P_{33} & 0_{3\times 3} \\ 0_{3\times 3} & P_{44}\end{bmatrix},\qquad P_{33}=\left(30\times 10^3\right)^2\times I_{3\times 3},\qquad \text{and}\qquad P_{44}=26^2 I_{3\times 3},\qquad P_{22}=\begin{bmatrix} P_{55} & 0_{4\times 3} \\ 0_{3\times 4} & P_{66}\end{bmatrix},$$

$$P_{55}=\left(\frac{1}{3}\right)^2\times I_{4\times 4},\ P_{66}=\left(\frac{2}{3}\times\frac{1}{\Delta T}\right)^2\times I_{4\times 4},$$

The estimation error of attitude angles is shown in Fig.10. As clear in this figure, the estimation error is converging to near zero within about 10 seconds despite large initial attitude estimation error. Fig. 11 shows the angular velocity estimation error. Fig.12 shows the position estimation error between the true and estimated satellites. Fig.13 shows the magnitude of the position estimation error between the true and estimated satellites. As shown in this figure the estimation error is reduced drastically before 5 seconds. The maximum standard deviation of the attitude angles estimation error was 0.029º. The standard deviation of the magnitude of the position estimation error is about 10.85 m.

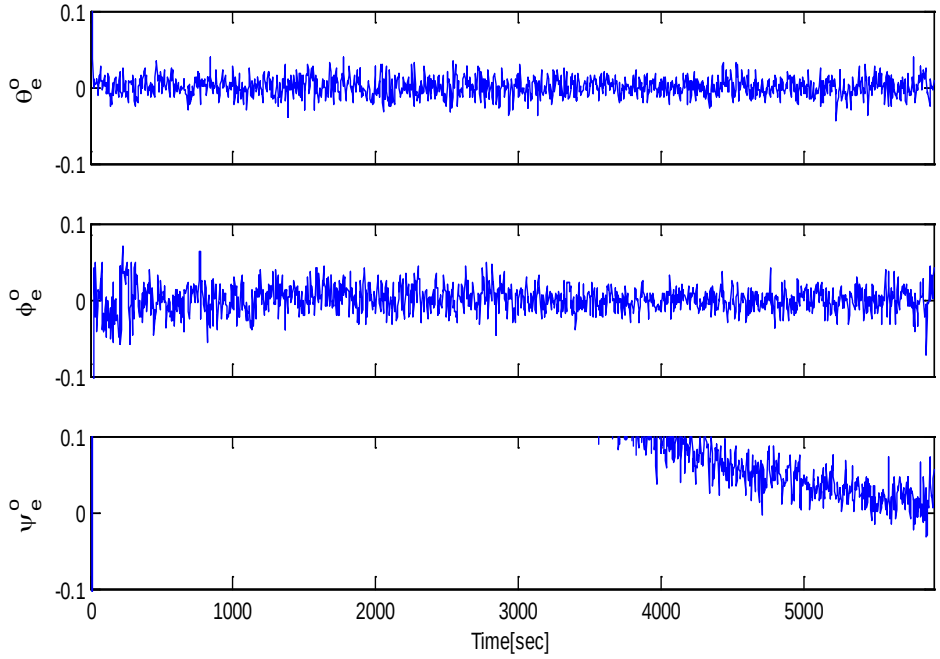


Fig. 10. Attitude estimation error.

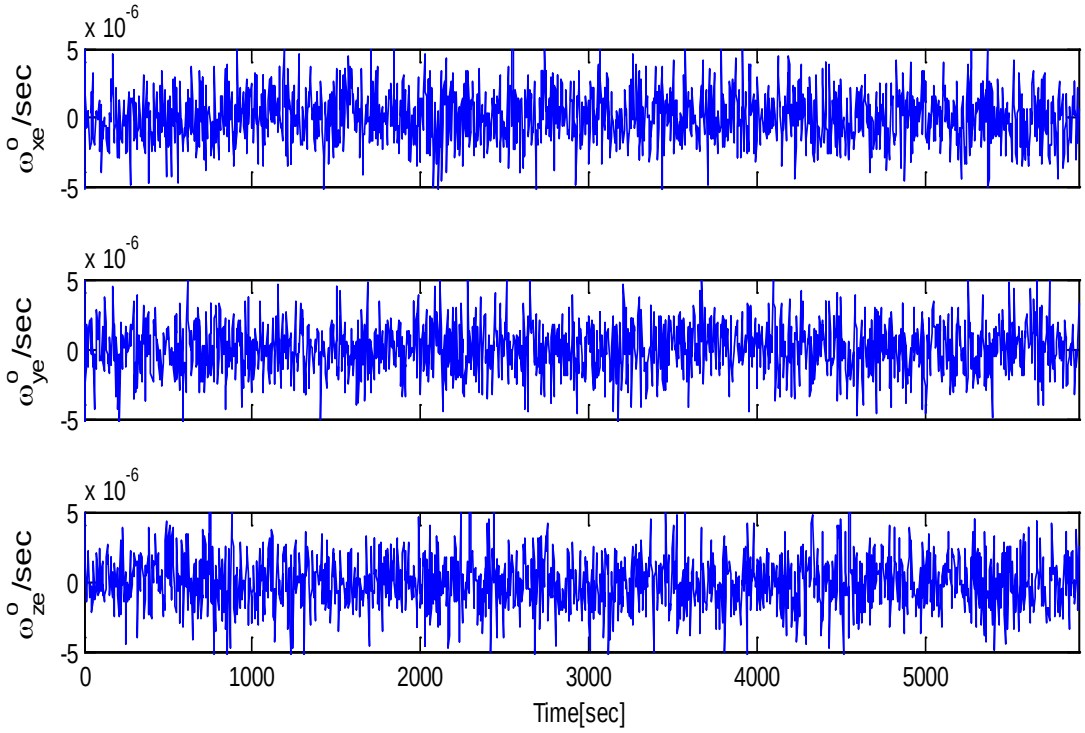


Fig. 11. Angular velocity estimation error.

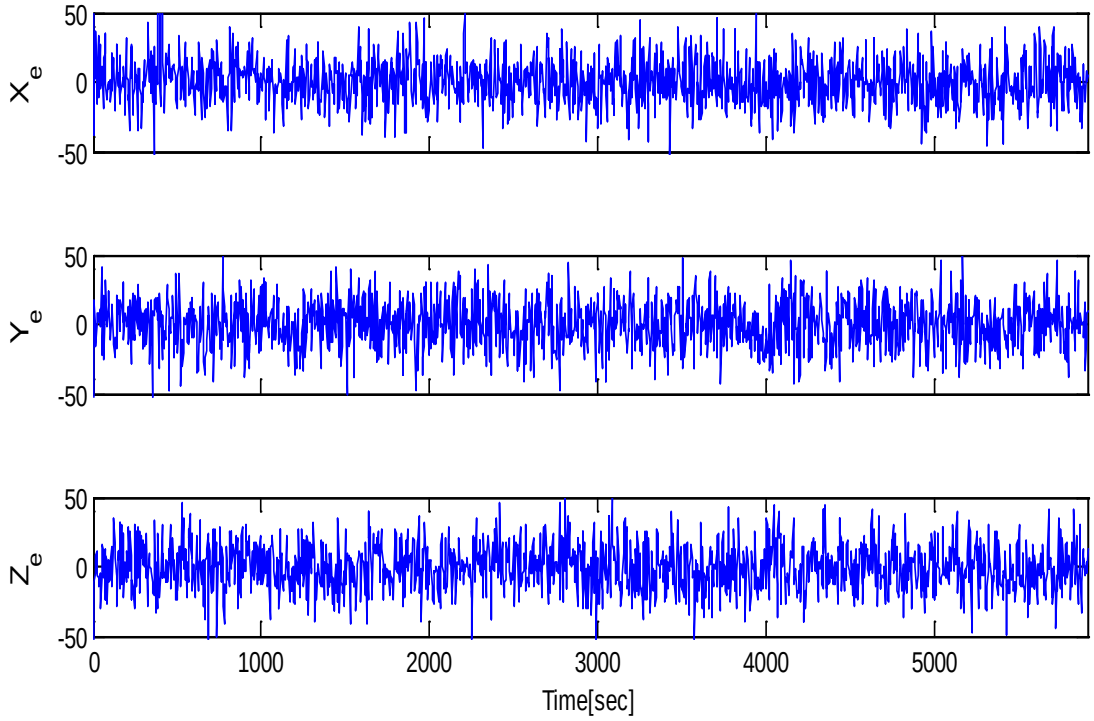


Fig. 12. Position estimation error.

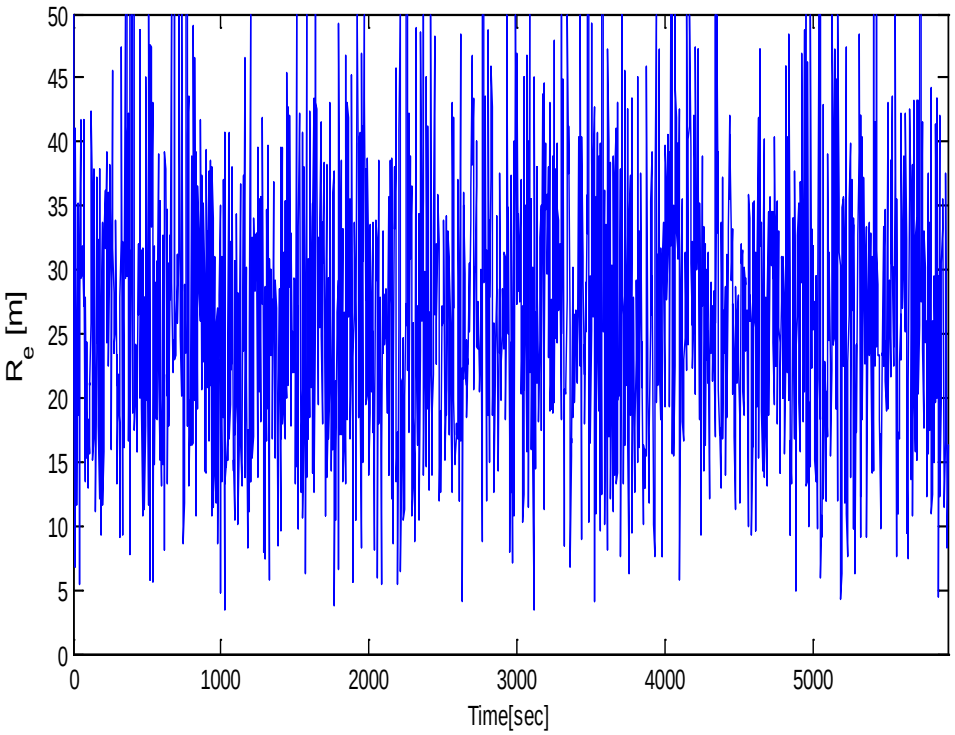


Fig. 13. Magnitude of position estimation error.

**2.2 Onboard processors**

Onboard processors of currently flying spacecraft are usually not up to date as our desktop processors. For example, the processor of the former Egyptian satellite, EGYPTSAT-1, was 386. This processor dates back to the 80's. On Dec, 2014, Shron, G. wrote [32] "Orion, NASA's next-generation deep space vehicle, is going to

eventually fly to Mars - run by a computer that's no smarter than your smartphone. Orion, whose launch this morning was delayed until at least Friday, doesn't carry state-of-the-art computers and its processors are 12 years old". Even the double-cored developed by Tubitak Uzay [33], has not yet obtain proven history of flight records on-board several missions.

## III. SOFTWARE

The software components of the attitude and orbit monitoring system are divided into management software and state estimation software. The management software monitors and controls the attitude and orbit sensors. The data coming from attitude and orbit sensors enables the processor to deal with different faults according to the applied Fault Detection, Isolation, and Recovery (FDIR) algorithm [47]. The discipline of fault management (FM), could be considered as a parent of FDIR. FM is the study of how the system could deal with faults. The FDIR mechanism determines the fault occurrence, fault type, and location and takes the appropriate recovery action [34]. There are several languages to develop FDIR algorithm such as Universal Modelling Language (UML) [46], its extension, System Modeling Language (SysML), and Architecture Analysis & Design Language (AADL) [50].A model-based FDIR algorithm contains models of the sensors and the process (which is the spacecraft itself) in order to generate residuals. The residuals are coming from sensors' noise and faults. Fault detection and isolation, (FDI), uses these residuals to identify fault existence, and fault source. The residuals could be computed by the difference between the measured and estimated outputs. Fault detection and diagnosis (FDD) represents an intermediate step between FDI, and FDIR. The FDI estimates the fault effect and diagnosis its severity. For, AOCS, fault identification is a very complex problem, and sometimes may be tricky. This will be shown in the following case study. The COMPASS is a toolset which automates current manual procedures of analyses. This toolset could be used to evaluate the effectiveness of FM.

**Case study:**

Our case study is based on that of [34], chapter six. The author of [34] presented Fig.10 to clarify his case study.

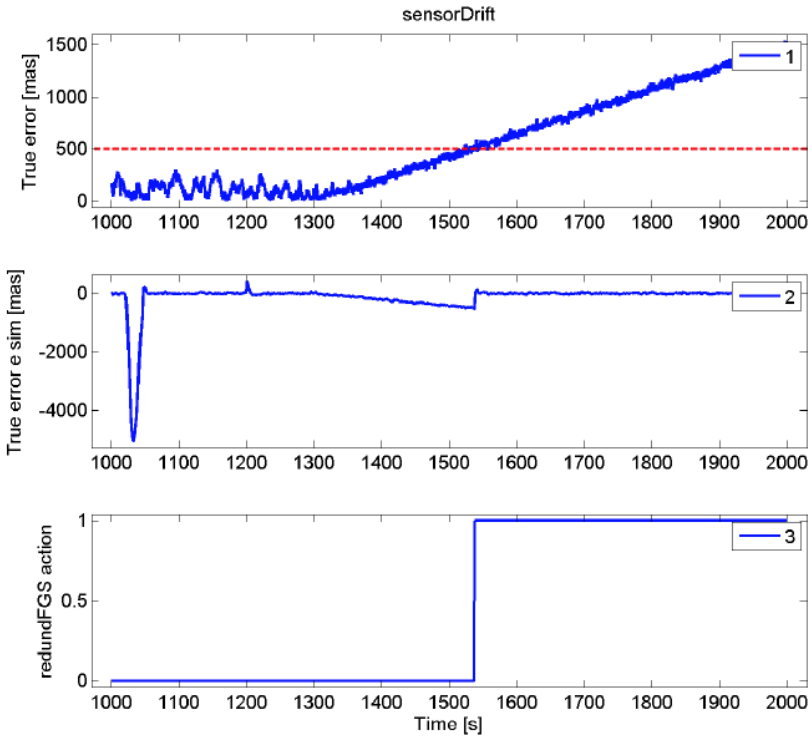


Fig. 14. Residual monitor signal, attitude error angle, and recovery action respectively.

The author assumes two identical sensors, A, B. The main sensor, A, starts to provide erroneous signal due to injected bias (sensor drift). Sensor drift fault is injected at time 1200 sec. This is represented by a small peak in the first plot of Fig. 10, at time 1300 sec. The error of sensor A begins to grow. The author then identifies a threshold level of the sensor error (The red dashed line in the first plot of Fig. 14) and then takes the recovery action. The recovery action started approximately at time 1550 sec as indicated by the third plot of Fig. 10. The recovery action is to switch the redundant sensor, B. Sensor error is defined as the difference between the measurements of sensor, A, and B. Sensor B, is inherently assumed to be without any fault, and here is the trick

that the author fallen into. Actually, Error growth may be because sensor B, started to exhibit sensor drift. Thus, sensor B, is the source of fault, not sensor A, and this situation could easily be encountered. To solve this issue, we must go further some steps beyond the steps done by the author of [34]. Without loss of generality, let's assume that sensor A, is a magnetometer which, as stated earlier in this review article, measures the earth's magnetic field vector.

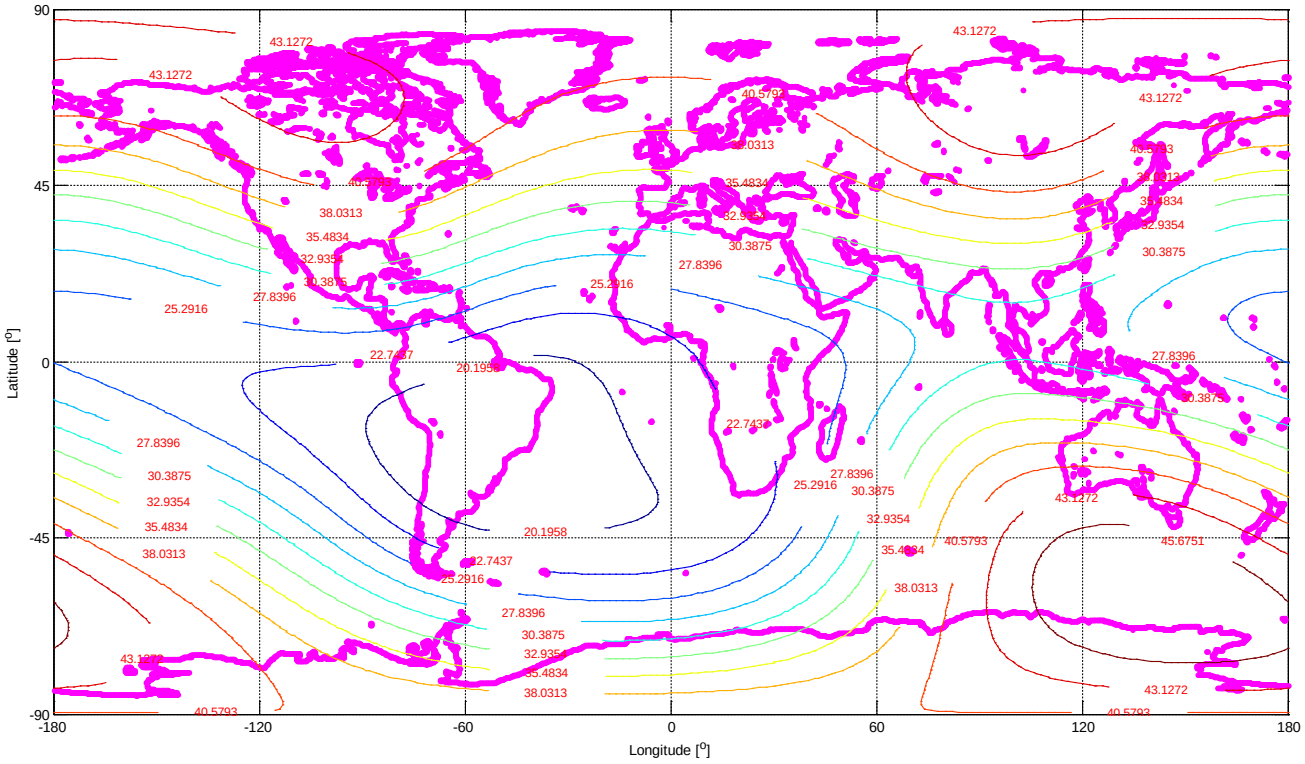


Fig. 15. Earth's magnetic field magnitude at 688 km altitude ($\mu$ Tesla).

The residual (error signal) must be now defined as the difference between the magnitudes of the measured earth's magnetic field vector measured by sensor A, and the predicted value of the earth's magnetic field vector magnitude. The predicted value of the earth's magnetic field magnitude could be determined from an on-board simulator of the earth's magnetic field. This model must be on-board any spacecraft which uses magnetometer.

Fig.15 presents the contours of the earth's magnetic field vector magnitude at an altitude of 668 Km which is corresponding to the altitude of the former Egyptian scientific satellite EGYPTSAT-1. If the position of the spacecraft is determined by any other sensor (such as GPS, radar, optical telescopes, or any other means), then the magnitude of the estimated earth's magnetic field could be calculated based on the on-board simulator. For example, if the satellite is flying over Cairo, the magnitude of the estimated earth's magnetic field magnitude is 30.3875 ($\mu$ Tesla), as shown in Fig. 15. If the sensor noise level, which is given by the manufacturer is about 200 nT, then the predicted sensor output will be approximately 30.39±0.2 nT. Thus, a reasonable upper threshold value at Cairo could be 30.65 nT, and the lower threshold value could be 30.1 nT. Thus, if the residual is greater than ±0.2 nT, the redundant sensor, B, should be triggered. We should also recall that the residual threshold value must be enlarged to a value of ±0.1 nT sometimes to account for disturbances affecting the earth's magnetic field. These disturbances are mainly due to solar wind, and solar flares [8].

Solar wind is neutral plasma emitted by the sun. This wind compresses the earth's magnetic field forming a shock front as seen in Fig. 16 [35], and [36]. The solar wind is sometimes associated with energetic plasma gusts produced by solar flares. This case study shows clearly how much complexity is associated with the usage of attitude monitoring hardware. It is a multidisciplinary problem that need a team work of specialists. The problem at hand needs to be solved by and AOCS specialist, space environment specialist, and FM specialist. Ref. [37] represents a good survey over FDIR strategies on-board spacecraft.

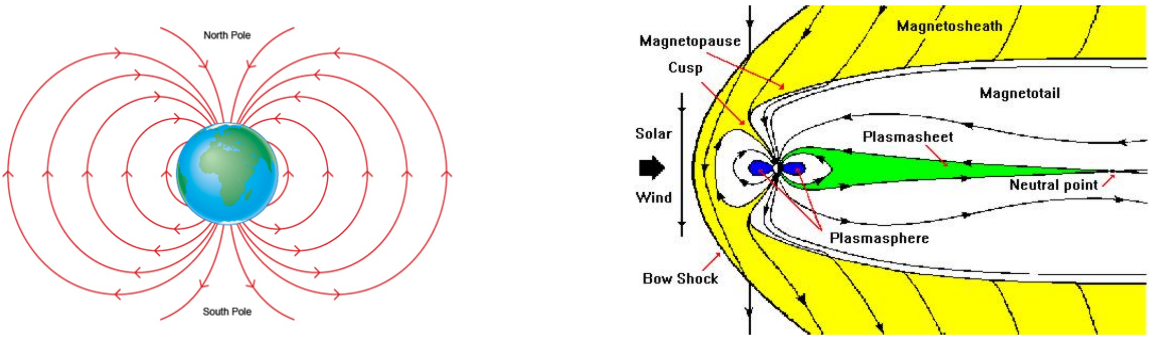


Fig. 16. Magnetic field compression due to solar wind.

State estimation: The problem of spacecraft attitude and orbit monitoring is considered to be a complicated process. The state estimation process is divided into 4 main sub-tasks. The first sub-task is the task of spacecraft attitude and orbital motion model. Ref. [12] presents a survey over various models of spacecraft attitude and orbital motion models. Dealing with sensors usually complicates the state estimation process. Many sensors don't provide directly the desired quantities such as spacecraft attitude angles and position in orbit. Clear examples of these sensors are magnetometers and sun sensors. The process of extracting the required quantities from a magnetometer and a sun sensor is considered to be an art. Ref. [12] presents various models associated with each type of sensors. In addition, using such sensors requires modeling of the space environment. Referring to Fig. 1, the determination process is conventionally considered with the attitude monitoring sensors. If the number of physical quantities to be measured is greater than or equal two, then we could use either attitude determination algorithms, or attitude estimation algorithms. Attitude determination algorithms are usually simpler, and faster than attitude estimation algorithm. But they don't make use of spacecraft model at all. If the number of the measured physical quantities is less than two, or if high accuracy levels of attitude and orbit monitoring is required, then we have no choice other than to use estimation algorithms. Sensor misalignment, colored noise, bias, and bias drift are also problem which could be solved only by estimation algorithms. Similarly, if the spacecraft consumes fuel during its orbital or attitude motion, then the spacecraft inertia matrix must be identified on-board the spacecraft due to the change of inertia characteristics caused by the fuel mass distribution change. Estimation algorithms make use of spacecraft models and measurements of sensors at the same time. They optimally mix the predictions of spacecraft attitude and orbit based on spacecraft models with the measurements coming from various types of sensors to provide a best estimate of the spacecraft attitude and orbital motion. The second source of complexity is the limited mass, and power budgets of spacecraft, and high cost of launching per kg mass which could range approximately from 4000 to 14000 $/kg [38].

## IV. RELIABILITY

At first glance, increasing the reliability of an AOCS is thought to be achieved by increasing the number of redundant components, which in turn increases the cost. A proper design of the AOCS may achieve the desired reliability with minimum cost increment. Thus, it is an optimization problem. Reliability has a close relation with probability because reliability of an AOCS is defined as the probability that the AOCS will function as expected. The probability of an event, *P(A)* satisfies the axiom [3]

$$0 \le P(A) \le 1 \tag{1}$$

Thus, 1 is an upper bound of the probability. If an event A, and B, are mutually exclusive, then

$$P(A \cup B) = P(A) + P(B) \tag{2}$$

And if A and B are not mutually exclusive, then

$$P(A \cup B) = P(A) + P(B) - P(A \cap B) \tag{3}$$

P(A/B): Conditional probability of event A occurrence if event B occurred. If the failure density function, $f(t)$, exists, then the probability of failure occurrence by time t is given by,

$$F(t) = \int_0^t f(t)dt \tag{4}$$

The reliability of the AOCS is working properly without failure is then given by

$$R(t) = 1 - F(t) \tag{5}$$

If the failure rate, $\lambda$, is constant with time (i.e., It is not affected by equipment age), then the exponential distribution of reliability is given by

$$R(t) = e^{-\lambda t} \tag{6}$$

The probability of having at least one failure by time $t$, the failure distribution function, is

$$F(t) = 1 - R(t) = 1 - e^{-\lambda t} \tag{7}$$

Accordingly, the failure density function is

$$f(t) = \frac{dF(t)}{dt} = \lambda e^{-\lambda t} \tag{8}$$

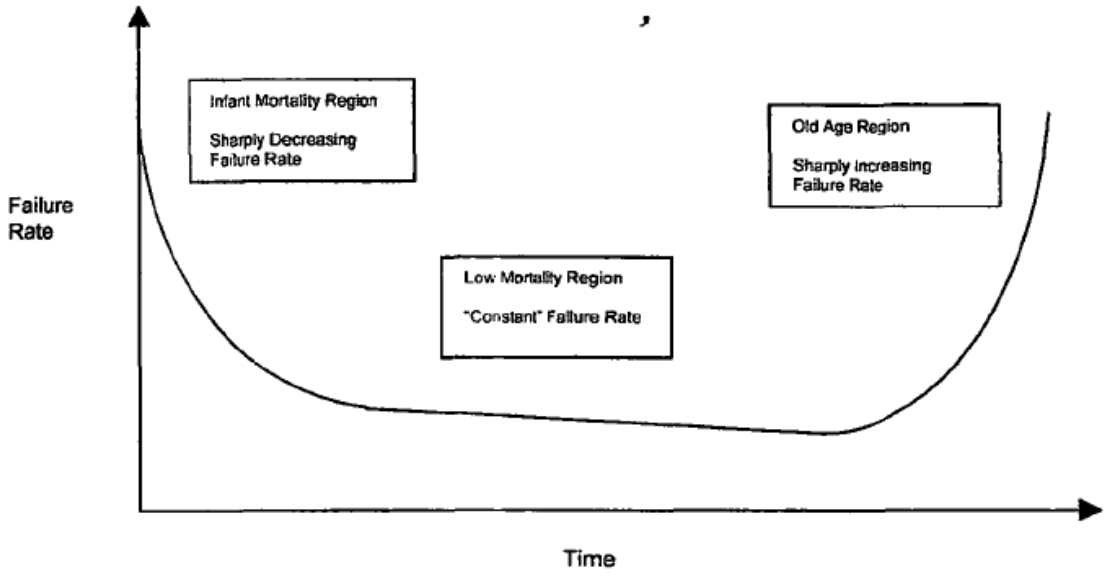


Fig. 17. Bathtub reliability curve

During the life time of the AOCS, there are different failure rates experienced as shown in Fig. 17, which is known as (Bathtub curve). The initial AOCS failure rate, according to Fig. 13, is high and decreasing rapidly. This zone is called infant mortality zone. After this region, the approximately constant failure rate region comes. This region is called also low mortality region. The third region is the old age region which is characterized by sharply increasing failure rates. The main objective of AOCS testing is to ensure that all of the components have operated long time enough to pass the infant-mortality region. Non-constant failure rate systems are commonly known as Weibull distribution. The corresponding failure distribution function is

$$F(t) = 1 - e^{-\left[\frac{t-t_0}{\tau-t_0}\right]^{\beta}} \tag{9}$$

Where τ is the Mean Time Between Failure (MTBF), so

$$\tau = \frac{1}{\lambda} \tag{10}$$

The constant, $\beta$, is known as the Weibull modulus. If $\beta < 1$, then the hazard rate decreases with time. This means that, as the system gets older, its failure rate decreases. If $\beta = 1$, then it is the constant failure-rate law. If $\beta > 1$, then the system is in the infant mortality region, or the old mortality region.

**Case studies (Reliability of series and parallel systems):**

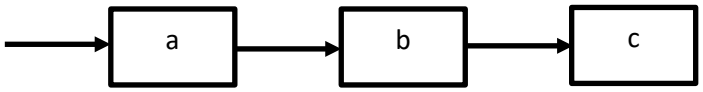


Fig. 18. Reliability of series components.

The series probability, $R_s$, of the components shown in Fig. 18, is given by

$$R_S = R_a R_b R_c$$

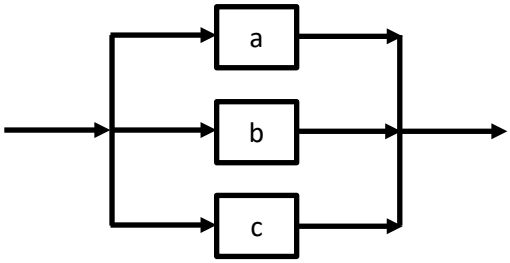


Fig. 19. Reliability of parallel components.

The overall reliability of the parallel components shown in Fig. 19 is given by

$$Rp = 1 - (1 - R_a)(1 - R_b)(1 - R_c)$$

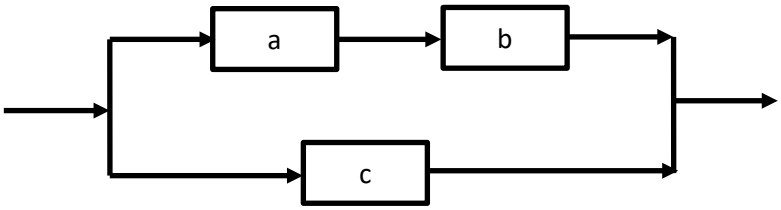


Fig. 20. Full redundants but not identical.

The reliability of the system shown in Fig. 20 is calculated from

$$R = 1 - (1 - R_a R_b)(1 - R_c)$$

Ref. [41] defines failure as an incident leading to temporarily or permanent mission degradation. Failure definition is an important process required when we speak about reliability. Failure analysis in [41] is studied based on 129 different spacecraft flown from 1980 to 2005. Damage magnitude is measured by two criteria, namely, loss of mission, and mission degradation. A mission is considered to be lost when a failure prevents the spacecraft to fulfill the primary mission objectives. A mission is considered to be degraded when a portion of the mission objectives is abandoned temporarily or permanently.

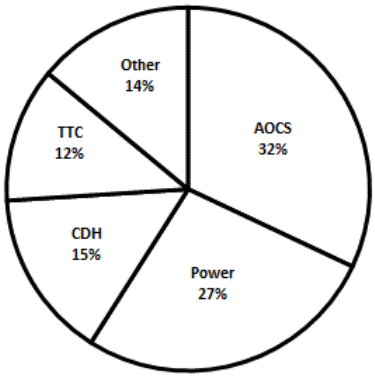


Fig. 21: Spacecraft failure due to different subsystem.

As shown in Fig. 21, the AOCS is responsible for 32% of spacecraft failures. Failure types are classified as mechanical, electrical, software, and unknown. AOCS consists of mechanical, electrical, and software. In Ref. [41], the percentage of electrical failures is higher than that of mechanical failures. We could think that electrical components have longer life times than mechanical components. But we must also consider that there are much more electrical components than mechanical parts which in turn increases the percentage of electrical failures.

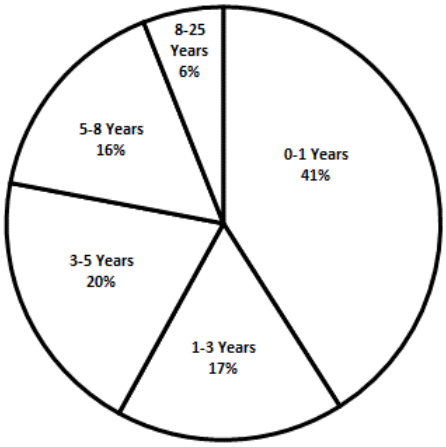


Fig. 22. Time to failure.

Fig. 22, shows that most failures occur in the first year of operation. Recalling Fig. 13, this time region is called infant mortality region. Spacecraft failure in this time region indicates insufficient testing as mentioned earlier in the current article.

Fig. 23 shows AOCS failure types. As shown in this figure, mechanical failures are responsible for 54% of AOCS failures. Fig. 24, shows the time to failure for AOCS.

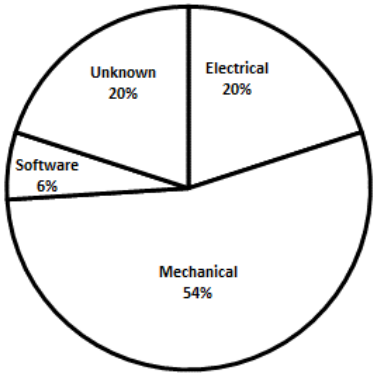


Fig. 23. AOCS failure types

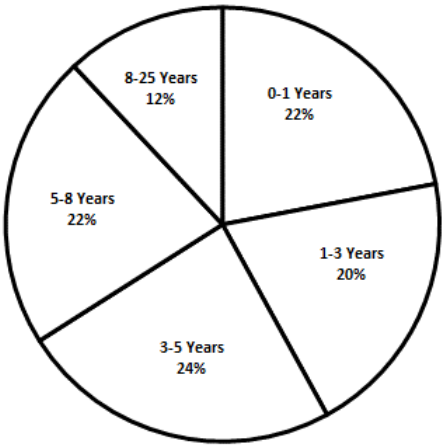


Fig. 24. AOCS time to failure.

The behavior of AOCS failures shown in Fig. 18 has 20% of unknown failure reasons due to lack of information. Also more that 50% of system failures is due to actuators, and not for the monitoring system of attitude and orbit. The AOCS has the lowest ratio of failures during the first year of operation. Special redundancy procedures could also extend the AOCS lifetime considerably. Software and hardware flexibility are important. The BeppoSAX and ERS2 AOCS software flexibility allowed the operators to upload a gyroless attitude control algorithm after failure of gyros. The star tracker handling software of BeppoSAX spacecraft was completely redesigned. Flexibility of EchostarV, and Radarsat-1 AOCS also increased their lifetime. Ref. [4] discusses some reliability analysis for Attitude Control Subsystem (ACS) not AOCS. The nonparametric ACS reliability analysis showed that the ACS reliability best estimate falls to about 98.4% after 11 years of operation. The actual reliability of the ACS falls between 97.5% and 99.3% at the same period based on (95% likelihood). During the first year of operation, reliability decreases sharply, indicating infant mortality behavior. The, old age (wear out) behavior, is represented as a decrease of reliability after 5 year on-orbit. The parametric analysis for ACS failure data showed that, the maximum likelihood estimate (MLE) of a single Weibull distribution is given by the relation

$$R(t) = e^{-\left[\frac{t}{3831}\right]^{0.7182}} \tag{11}$$

The Weibull modulus (0.7182) is less than 1. The single Weibull distribution could not fully describe the dynamics of failure in the time region from 5 to 10 years. So a mixture distribution is provided by the following relation

$$R(t) = 0.9893e^{-\left[\frac{t}{258859.3}\right]^{0.4759}} + 0.0107e^{-\left[\frac{t}{9.8}\right]^{3.7142}} \quad (12)$$

The first Weibull modulus (0.4759) controls the infant mortality region, and the second Weibull modulus (3.7142) controls the wear out region. 11 % of spacecraft failures in the first year of their lifetime is due to ACS. This percentage starts to increase around year 6 indicating wear out failures of ACS. This percentage reaches 20% by year 15.

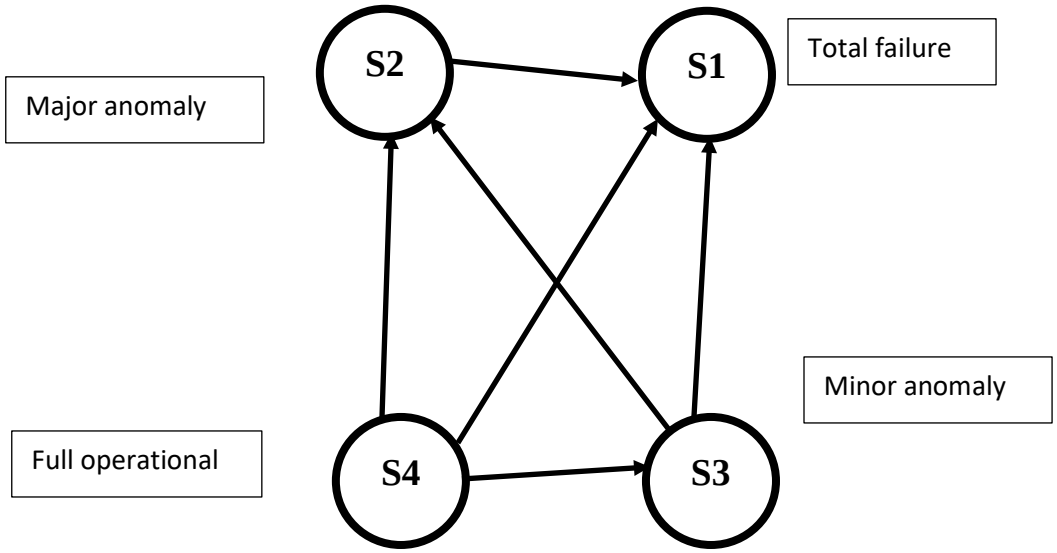


Fig. 25. Transition diagram and multi-state for AOCS.

Fig. 25 shows the transition diagram and multi-state for AOCS. Multi-state failure analysis introduces partial failures and degraded states not only a single failure state [43], [49]. After 15 years of operation, the reliability of certain component may be 98%, bt the probability of being fully operational is only 89%. The probability of being in minor anomaly is about 6%, in major anomaly, 3%, and total failure, 2%. The failure rate us usually measured with the unit FIT (failure event per 109 hours). Fault Tree Analysis (FTA) is a very helpful tool to analyze risk and reliability. A sample fault tree is shown in Fig. 26 [42].

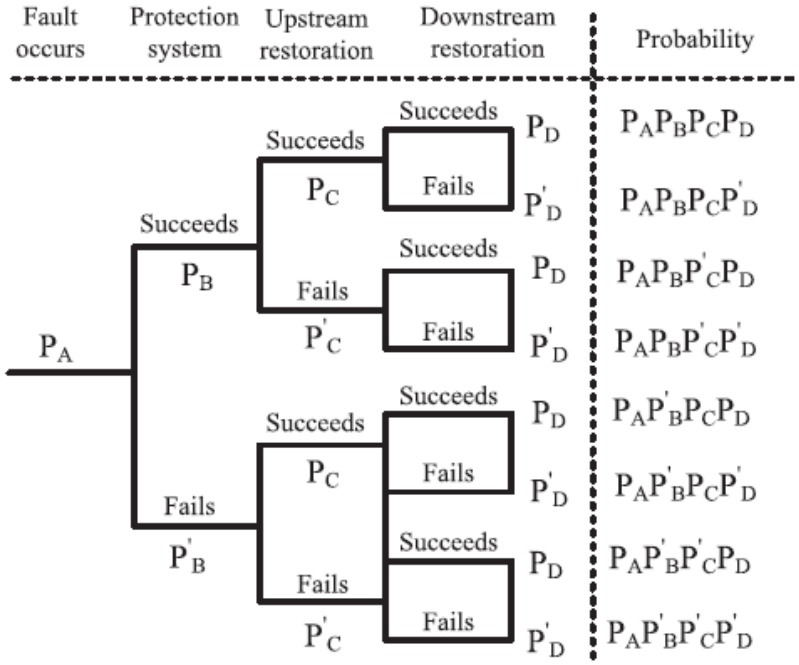


Fig. 26. A sample fault tree.

An intelligent Fault Tolerant system without hardware redundancy is discussed in [44]. Prediction of system reliability also could be established through many prediction algorithms and mathematical models. These methods could be categorized into [45]:

a- Model-Based Methods: these models select an adequate probability function as reliability model. This model could be used to predict future reliability. There are different approaches for these models such as Bayesian approach, and Non-Homogeneous Poisson Process (NHPP). The word RAMS stands for Reliability, Availability, Maintainability, and Safety [48]. RAMSAS is a model-based method through which reliability analysis for systems could be achieved by simulation.

b- Time series analysis: This method expresses reliability as a time series to predict the reliability. There are also different approaches also for these models such as autoregressive integrated moving average (ARIMA), a multilayer feed-forward neural network model (MFNN).

c- Machine learning: Recently, machine learning techniques have been used for reliability prediction. Feed-forward multilayer perceptions (MLP) network can identify underlying failure distribution and estimate the parameters. Expert systems based on neural networks could also be utilized in addition to hybrid learning neuro-fuzzy systems [51], generalized regression neural network model (GRNN), genetic programming (GP), and support vector machine (SVM) with simulated annealing. The optimal parameters for support vector regression (SVR) machine are obtained using real-value genetic algorithm.

d- Evidential reasoning (ER): This method is developed on the basis of decision theory. It could deal with linguistic terms such as “high”, “low”, “very high”, and “very low”.

## V. COST EFFECTIVENESS

The cost of an attitude and orbit monitoring system is due to several contribution resulting from many factors. This cost is divided into:

a- Hardware cost.
b- Software cost.
c- AOCS design cost.
d- AOCS assembly, integration, and testing cost.
e- Ground station operation cost [39].
f- On-board power and processing cost.
g- Launch cost.

Thus, a traditional reliability designer tends to increase the reliability by using redundant components. For spacecraft, this tendency is a disaster. To show the idea, assume that the designer wants to add a full redundant attitude and orbit monitoring sensor such as a GPS receiver that could be used to provide attitude and orbit measurements. First, the hardware cost of the sensor is doubled. Thus, 300 k $ are added initially to the cost. If the designer decided that the redundant sensor has a hot redundancy, then this sensor will be on. This will in turn increase the required power budget. This implies larger battery size, and weight to store more electric energy in addition to larger solar cells to generate the required power. The processing requirements increase also, implying more powerful processor which in turn may weight more and uses consumes more power. Thus, again, increasing the battery size and weight. Due to the increased mass, more powerful actuators are needed. These actuators cost and weight more, and requires more power to be generated by the Power subsystem. As stated earlier in this review article, this implies more testing time to pass the infant mortality stage. The redundant sensor needs to be mounted inside the spacecraft structure. Consequently, the size and weight of the structure is increased. This increment also will require more expensive, heavier, and more power consuming actuator. The assembly and integration cost also of such more complicated systems increases. The on-board and ground station software may also need to be changed to account for all of these changes. Take also into account that the total weight of the spacecraft now has been increased considerably. Which means of, course, more launching cost. I think now the situation is clear. The designer has fallen into the dilemma of increased size, power, cost and weight. This may lead the whole spacecraft mission to be not feasible at all. Thus, cost effectiveness needs some tools for cost estimation methods in order to be able to evaluate cost optimality for a certain design of an attitude and orbit monitoring system. Ref. [40] reviews hardware cost estimation methods and models. Traditionally, design effectiveness is considered to be done through maximizing the performance by reducing spacecraft weight. This concept now is considered to be outdated. The cost of space mission now is considered to be a new design criterion for management decision. The need for cost engineering and cost control are now considered as key constituent. At prephase-0/A, a preliminary cost estimate could determine if a certain design is achievable within the available cost or not. Cost estimation is thought of as a part of the cost engineering. Cost estimation is defined as the process of forecasting a product cost. The cost is a dynamic variable which must be always updated. It is not a constant or static variable. There are various cost models for subsystems and space instruments (SICM, NICM, MICM), for operations and processing (SOCM, MESSOC),

in addition to ground development and risk assessment (ACEIT, Crystal Ball, @Risk). For many missions, commercial off the shelf (COTS) components of the attitude and orbit monitoring are employed. Cost estimating relationships (CERs) relate subsystem cost to performance, and technical parameters. Date base quality and size for various components determine CER reliability. So, the data base must be updated to reflect new technologies, and requirements. Cost Estimation methods (CEMs) are: parametric cost estimation, engineering build-up estimation, analogy estimation, Expert judgment estimation (EJ), and Rough order of magnitude estimation (ROM). Once a cost estimation model is developed, a tool to implement this model is to be developed.

Cost life cycle include three phases: development, production, and operation. There are numerous tools those have been developed for cost estimation, such as Small Satellite Cost Model (SSCM), Price-H, True Planner, SEER®-H. Some of these tools are free, and others require annual fee for license renewal. For example SSCM is a free tool based on Microsoft Excel to provide ease of use. There are also several cost estimation reports, handbooks, and guides such as NASA Cost Estimating Handbook, ISPA Parametric Estimating Handbook, DoD Parametric Cost Estimating Handbook, and GAO Cost Estimating and Assessment Guide. It is also possible to use any combination of these models, and tools to obtain an AOCS cost estimate.

## VI. SUMMARY AND CONCLUSION

Spacecraft attitude and orbit monitoring process is of crucial importance. Once the spacecraft goes into space, it never comes back for repair. Thus, hardware failure or faults in most cases are not repairable. This monitoring process requires some form of integration among hardware and software components. Hardware components include sensors, processor, and interfaces for power and data transfer. Software components include estimation (& or) determination algorithms in addition to management software which applies the predefined FM actions. The monitoring process also in most cases is characterized by complex algorithms due to the complicated nature of the measurements. Usually, the sensors utilized do not provide the required information. Thus, a tremendous effort is exerted to extract the required information from measurements provided by sensors. Space operation also requires high reliability of software and hardware components. Due to limited spacecraft mass, power, and communication budgets in addition to high cost, some traditional reliability increasing methods (such as full redundancy) may not be appropriate. Critical subsystem components must be identified in order to increase their reliability. While trying to increase the reliability of critical components, we must pay a special attention for cost effectiveness. Estimation cost methods help the designer to achieve a cost effective design that guarantees mission feasibility.

## VII. ABBREVIATIONS

| | |
|---|---|
| AADL | Architecture Analysis & Design Language |
| AOCS | Attitude and Orbit Control system |
| ACS | Attitude Control Subsystem |
| ARIMA | Autoregressive Integrated Moving Average |
| CEMs | Cost Estimation Methods |
| CERs | Cost Estimating Relationships |
| DoD | Department of Defense |
| EJ | Expert Judgment |
| ER | Evidential Reasoning |
| FDD | Fault Detection and Diagnosis |
| FDI | Fault Detection and Isolation |
| FDIR | Fault Detection, Isolation, and Recovery |
| FIT | Failure Event per 109 hours |
| FM | Fault Management |
| FOG | Fiber Optic Gyro |
| FTA | Fault Tree Analysis |
| GNSS | Global Navigation Satellite Systems |
| GP | Genetic Programming |
| GPS | Global Positioning System |
| GRNN | Generalized Regression Neural Network Model |
| IC | Integrated Circuit |
| IMU | Inertial Measurement Units |
| MEMS | Microelectromechanical Systems |
| MFNN | Multilayer Feed-Forward Neural Network Model |
| MLE | Maximum Likelihood Estimate |
| MLP | Multilayer Perceptions |

| | |
|---|---|
| MTBF | Mean Time Between Failure |
| NHPP | Non-Homogeneous Poisson Process |
| nT | Nano Tesla |
| ROM | Rough Order Of Magnitude Estimation |
| SSCM | Small Satellite Cost Model |
| SVM | Support Vector Machine |
| SVR | Support Vector Regression |
| SysML | System Modeling Language |
| UML | Universal Modelling Language |

## VIII. ACKNOWLEDGMENTS

The author would like to thank Eng. Ashraf Adel, Eng. Abd El Salam Ramadan, Ahmed Abd ElMegeed, Dr. wael Murtada, and Dr. Tarek Nada for the resources they provided during the preparation of this review article.

## REFERENCES

[1] "IEEE Standard Dictionary of Electrical and Electronics Terms", New York: Wiley Interscience, 1984.
[2] Wertz, J. R., and Larson, W. J., "Spacecraft Mission Analysis and Design", Microcosm, Inc., 1999.
[3] Griffin, M.D., and French, J.R. "Space Vehicle Design", American Institute of Aeronautics and Astronautics, Inc, Second Edition, 2004.
[4] Jessica, K., Castet, J., and Saleh, J. "Spacecraft attitude control subsystem: Reliability, Multi-State Analyses, And Comparative Failure Behavior in LEO and GEO", Acta Astronautica, Vol.85, 2013, pp. 83-92.
[5] Bate, R. B.,and White, J. E., " Fundamentals of Astrodynamics", Dover Publications, Inc.,1971.
[6] Vallado, D., "Fundamentals of Astrodynamics and Applications", McGraw-Hill Companies, Inc., Second Edition, 1997.
[7] Montenbruck, O., Gil, E., "Satellite Orbits Models, Methods, Applications", Springer, Third Edition, 2005.
[8] Wertz, J. R., "Spacecraft Attitude Determination and Control", D. Reidel Publishing Company, 1997.
[9] Habib, T., "The Global Positioning System Application to Satellite Position and Attitude Determination", MSc thesis, Aerospace Department, Cairo University, 2003.
[10] Habib, T., A.H., Kassem, and G. M., El-Bayoumi, "GPS-Based Small Satellite Position and Attitude Determination Simulator", Journal of Engineering and Applied Science, Vol. 52, No. 1, 2005, pp. 71-87.
[11] Habib, T., S.D., Hassan, and G. M., El-Bayoumi, "Spacecraft Attitude and Attitude Rate Estimation Using Hybrid Kalman Filtering of Magnetometer Measurements", Proceeding of the 12-th International Conference on Aerospace science and Aviation Technology, 2007.
[12] Habib, T."New Algorithms of Nonlinear Spacecraft Attitude Control via Attitude, Angular velocity, and Orbit Estimation Based on the Earth's Magnetic Field", PhD Thesis, Cairo University, 2009.
[13] Habib, T., "Fast Converging with High Accuracy Estimates of Satellite Attitude and Orbit Based on Magnetometer Augmented with Gyro, Star Sensor and GPS via Extended Kalman Filter", The Egyptian Journal of Remote Sensing and Space Sciences, Vol.14, Issue 2, Dec. 2011, pp. 57-61.
[14] Habib, T., "A Comparative Study of Spacecraft Attitude Determination and Estimation Algorithms( A cost-benefit approach)", Aerospace Science and Technology, Vol.26, Issue 1, April-May, 2013, pp. 211-215.
[15] Habib, T., "Simultaneous spacecraft orbit estimation and control based on GPS measurements via extended Kalman filter", The Egyptian Journal of Remote Sensing and Space Sciences, Vol.16, Issue 1, 2013, pp. 11-16.
[16] Habib, T., "Concurrent Spacecraft Attitude and Orbit Estimation with Attitude Control Based on Magnetometer,Gyroscope, and GPS Measurements through Extended Kalman Filter", Journal of Basic and Applied Sciences, Vol. 10, 2014, pp. 461-468.
[17] Habib, T., "Combined Spacecraft Orbit and Attitude Control Through Extended Kalman Filtering of Magnetometer, Gyro, and GPS Measurements", The Egyptian Journal of Remote Sensing and Space Sciences, Vol.17, Issue 1, Jan, 2014, pp. 87-94.
[18] Afanasenko, M.P., "Attitude Determination and Control Subsystem. Magnetometer and Magnetometer GSE: Preliminary Design. Design Report", LC ISR, 2004.
[19] https://www.tindie.com/products/BBTech/mag3110-3-axis-digital-compass-magnetometer-module/
[20] LENS, J., "A Review of Magnetic sensors", Proceedings of the IEEE, Vol. 78, No. 6, June, 1990, pp. 973-989.

[21] http://www.cmosis.com/news/latest_news/cmosis_participates_in_esa_sun_sensor_on_a_chip_project.
[22] http://www.sciteclibrary.ru/eng/catalog/pages/951.html
[23] Mortari, D., “Moon-Sun Attitude Sensor”, Journal of Spacecraft and Rockets, Vol. 34, No. 3, May-June 1997.
[24] Danrongask, B." Development of Micromachined Electromechanically Suspended Gyroscope", PhD Thesis, University of Southampton, 2009.
[25] Samaan, M." Toward Faster And More Accurate Star Sensors Using Recursive Centroiding And Star Identification", PhD Thesis, Texas A&M University, 2003.
[26] http://www.ballaerospace.com/page.jsp?page=104.
[27] http://en.wikipedia.org/wiki/Global_Positioning_System.
[28] http://kobi.nat.uni-magdeburg.de/patrick/pmwiki.php?n=BEng.TheGPSReceiver.
[29] Itzhack Y. Bar-Itzhack, and Biton, I., “ Improved Direct Solution of the Global Positioning System Equation”, Journal of Guidance Control and Dynamics, Vol.21, No.1, 1998, pp. 45-49.
[30] Shorshi, G., Itzhack Y. Bar-Itzhack, “Satellite Autonomous Navigation Based on Magnetic Field Measurements”, Journal of Guidance Control and Dynamics, Vol.18, No.4, 1995, pp. 843-850.
[31] Naqvi. N., “Attitude Determination of Small Satellite Using Global Navigation Satellite System”, ISNET/TUBITAK UZAY Workshop on Small Satellite Engineering and Design for OIC Countries, Oct, 2014.
[32] http://www.computerworld.com/article/2855604/the-orion-spacecraft-is-no-smarter-than-your-phone.html.
[33] http://uzay.tubitak.gov.tr/sites/images/en_bilgegilgamis_tekyon.pdf.
[34] Homar, A., “AOCS Fault Detection, Isolation And Recovery: A Model-Based Dynamic Verification & Validation Approach”, MSc thesis, Luleå University of Technology, 2014.
[35] http://helios.gsfc.nasa.gov/magnet.html.
[36] http://www.bbc.co.uk/schools/gcsebitesize/science/21c/chemicals_in_our_lives/minerals_in_britainrev2.shtml.
[37] Wander, A. and Forstner R. “Innovative Fault Detection, Isolation and Recovery strategies on-board spacecraft: State of the art and research Challenges”, Deutscher Luft- und Raumfahrtkongress, 2012.
[38] Abd Elmageed, A., “Launchers”, National Authority for Remote Sensing and Space Sciences, Technical Report, Issue 3, 2014.
[39] Ha, J., Marshall, M., and Landshof, J., “Cost-Effective Mission Operations”, Acta Astronautica, Vol.39, No.1-4, 1996, pp. 61-70.
[40] Trivailo, O., Sippel, M., and Sekercioglu, Y., “Review Of Hardware Cost Estimation Methods, Models And Tools Applied To Early Phases Of Space Mission Planning”, Progress in Aerospace Sciences, Vol.53, 2012, pp. 1-17.
[41] Tafazoli M., “A Study of On-Orbit Spacecraft Failures”, Acta Astronautica, Vol.64, 2009, pp. 195-205.
[42] Ahadi, A., Ghadimi, M., and Mirabbasi, D., “Reliability Assessment For Components Of Large Scale Photovoltaic Systems”, Journal of Power Sources, Vol.264, 2014, pp. 211-219.
[43] Castet, J., and Saleh, J. “Beyond Reliability, Multi-State Failure Analysis Of Satellite Subsystems : A Statistical Approach”, Reliability Engineering and System Safety, Vol.95, 2010, pp. 311-322.
[44] Chandrasekar, S., et al. “An Intelligent Fault-Tolerant Satellite Attitude Control System with-out Hardware Redundancies”, 11th International Conference on Control, Automation, Robotics, and Vision, Singapore, 2010.
[45] Hu, C., Si, X., and Yang, J. “System Reliability Prediction Model Based On Evidential Reasoning Algorithm With Nonlinear Optimization”, Expert Systems with Applications, Vol 37, 2010, pp. 2550-2562.
[46] Pontuschka, M., and Fonseca, I., “FDIR for the IMU Component of AOCS Systems”, Mathematical Problems in Engineering, Vol 2014, 2014, pp. 1-9.
[47] Liddle, D., et al, “A Low-Cost Geostationary Mini-satellite Platform”, Acta Astronautica, Vol 55, 2004, pp. 271-284.
[48] Garro, A., et al, “Reliability analysis of an Attitude Determination and Control System (ADCS) through the RAMSAS method”, Journal of Computational Science, Vol 5, 2014, pp. 439-449.
[49] Castet, J., and Saleh, J. “On The Concept of Survivability, With Application to Spacecraft and Space-Based Networks”, Reliability Engineering and System Safety, Vol.99, 2012, pp. 123-138.
[50] Bozzano, M., et al, “Spacecraft Early Design Validation Using Formal Methods”, Reliability Engineering and System Safety, Vol.132, 2014, pp. 20-35.
[51] Patton, R., et al, “Robust FDI Applied to Thruster Faults of a Satellite System”, Control Engineering Practice, Vol.18, 2010, pp. 1093-1109.